LANGMUIR

Article

pubs.acs.org/Langmuir

# Infrared Absorption Enhancement by Charge Transfer in Ga-GaSb Metal-Semiconductor Nanohybrids

Yu Sun, Long Yuan, Xiaofeng Wu, Yingge Cong, Keke Huang, and Shouhua Feng*

State Key Laboratory of Inorganic Synthesis and Preparative Chemistry, College of Chemistry, Jilin University, Changchun 130012, PR China

Supporting Information

**ABSTRACT:** We fabricated Ga-GaSb nanohybrids by the droplet epitaxy method and precisely tuned the interaction between the metal and semiconductor parts. Selective absorption enhancement from 1.2 to 1.3 $\mu$m was confirmed via ultraviolet−visible−infrared absorption spectra in all of the nanohybrids, which shows size and component dependence. Valence band spectra of the samples indicate that carrier separation occurs at the interface at the Schottky junction and the high density of states near the Fermi level in a semiconductor controls the process of charge transfer. Thus, the enhanced selective absorption in the infrared region will open up a broad prospect for applications in infrared detection and thermophotovoltaic cells.

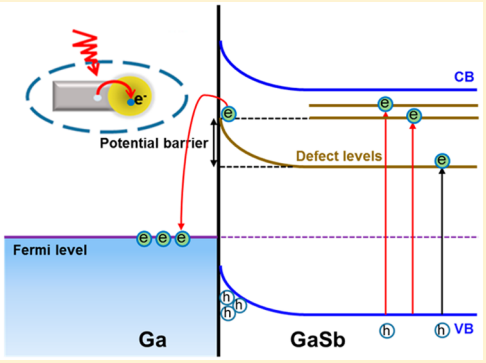


## INTRODUCTION

Metal-semiconductor (MS) hybrids, combination of different metal and semiconductor materials in a nanostructure, have attracted much attention for their availability to design the absorption and emission properties, control the nanoscale energy-transfer processes, create new excitations in the coupling regime, and increase the optical nonlinearities.[1−4] The interaction between the material components of hybrid nanoparticles is the key point for designing and modifying their properties. Precise control of the size and composition of nanohybrids makes it possible to satisfy different application requirements by tuning the interaction.[5] For example, the photoluminescence property of Au-CdS MS nanostructures may be promoted through a carrier transfer process;[6] for example, the excited electrons on the metal surface transfer via a surface plasmon wave to the conduction band of the semiconductor and recombine with holes in the valence band. The Schottky junction formed at the interface, an interaction between metals and semiconductors, controls the process of charge transfer. Its potential barrier strongly depends on the crystal facet of the semiconductor attached to the metal. Hence, the semiconductor crystal in the hybrid design may be better enclosed by a certain proper facet to promote its various performances. It was proved that the Schottky barrier can be formed at the $Cu_2O$ (100)-Pd interface to accelerate the migration of holes from $Cu_2O$ (111) to Pd for improved photocatalysis.[7]

It is reported that the core−shell structure of Cu@$Cu_2O$ could favor the charge transfer and inhibit recombination of photogenerated hole−electron pairs[8] and drive an enhancement of photocatalytic activity in the visible-light region. The tunable surface plasmon resonance absorbance from 568 to 761 nm was realized at the Ag-$Ag_2S$ heterojunction.[9] Most of these MS hybrids exhibit good performance in the visible-light region. Our motivation is to select a proper system in the infrared (IR) region.

III-Sb materials are attractive candidates as IR detectors due to their small band gap, ranging from 1.6 eV (AlSb) to 0.2 eV (InSb). In this work, we synthesized Ga-GaSb(111) MS nanohybrids by droplet epitaxy[10−13] to study the infrared absorption property. Their size mainly depends on the size of the metal drop initially formed by the Ga flux. Compared with the GaSb epi-film, absorption is enhanced, ranging from 1200 to 1380 nm in these MS nanohybrids, which is mainly caused by charge separation at the interface; namely, electrons transfer to the metal surface and holes gather into the valence band with the top bending upward. The process of charges transfer is confirmed by the density decrease of states (DOS) in the valence band spectrum. Thus, the Ga-GaSb nanohybrids will open up a broad prospect for applications in IR detection.

## EXPERIMENTAL SECTION

Prior to growth, p-type low-resistance Si(111) wafers doped with B were chemically cleaned by Shiraki clean procedures.[14] The cleaned wafers were immediately loaded into the molecular beam epitaxy (MBE) load-lock chamber and degassed at 200 °C under a final pressure of $5 \times 10^{-8}$ Torr for 2 h. A SVTA III-V reactor equipped with a valved cracking cell for Sb and an effusion cell for Ga was used to grow these nanohybrids. The cracking zone temperature of the Sb source was fixed at 1000 °C to provide atomic antimony and $Sb_2$. The base pressure maintained in the growth chamber was about ~$10^{-10}$

**Received:** February 19, 2016
**Revised:** April 8, 2016
**Published:** April 9, 2016

ACS Publications © 2016 American Chemical Society



DOI: 10.1021/acs.langmuir.6b00628
*Langmuir* 2016, 32, 4189−4193

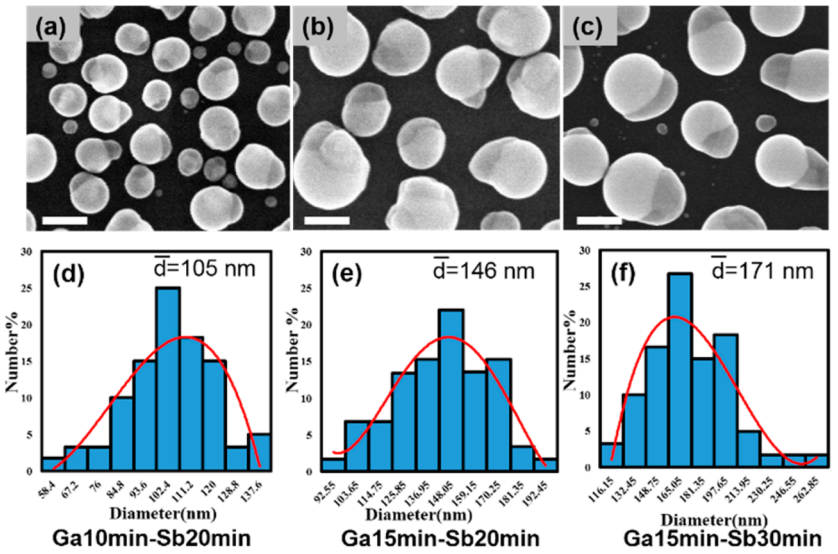


**Figure 1.** SEM images of the MS hybrids for samples A (a), B (b), and C (c). All scare bars are 100 nm. The corresponding particle size statistic graphs are showed in (d), (e), and (f).

Torr. The substrates were annealed at 800 °C for 10 min to get Si (111)-(7 × 7) reconstruction. Then the substrate was directly cooled down to 350 °C for the growth.

First, Ga droplets were formed by supplying Ga flux without Sb flux, and then these droplets were crystallized by supply of Sb flux. This method was used to obtain three samples of Ga-GaSb metal-semiconductor hybrid nanostructures with three different Ga and Sb flux duration times, and the only difference is the duration time of Ga and the Sb flux. The three samples were named as A (the duration time was 10 min for Ga and 20 min for Sb), B (the duration time was 15 and 20 min), and C (the duration time was 15 and 30 min), respectively.

Surface morphologies were analyzed with scanning electron microscopy (SEM) by FEI Helios Nanolab 600i. The hybrid nanostructures formed by two different phases of metal and semiconductor were confirmed by atomic force microscopy (AFM) (NSK SPA400) in phase scan mode. High-resolution transmission electron microscopy (HRTEM) (FEI Tecnai G2 S-Twin F20) was used to verify the crystal facet of GaSb attached to Ga metal. The solid ultraviolet−visible−infrared (UV−vis−IR) absorption spectrum within the wavelength 1100−1800 nm was obtained with a Shimadzu U-4100. X-ray photoelectron spectroscopy (XPS) (Thermo ESCALAB250) scanned the valence band spectrum to study the electronic structure near the Fermi level.

## RESULTS AND DISCUSSION

The surface morphologies of the Ga-GaSb metal-semiconductor nanohybrids grown on Si(111) substrates were characterized by SEM. Each nanohybrid consisted of two parts in different contrast and had a similar configuration with a bulb. The particle size statistics have been done with 100 particles, respectively, and detailed SEM images can be found in the Supporting Information (SI). The average size was about 105.23 nm, 146.76 nm, and 171.54 nm for samples A, B, and C, respectively. For sample A (Ga 10 min-Sb 20 min) and B (Ga 15 min-Sb 20 min), shown in Figure 1(a) and (b), the particle size of the nanohybrids increased with the duration time of the Ga flux at the cost of a decrease in density. Thus, the particle size strongly depended on the size of the metal drop initially formed by the Ga flux.[15] But the proportion of semiconductor obviously enlarged in sample C (Ga 15 min-Sb 30 min) in Figure 1(c). The height of the nanohybrids increased with its size as shown in AFM images in the SI. According to the XRD pattern in the SI, the hybrids consist of metal Ga and semiconductor GaSb. Phase diagrams were obtained simultaneously with the AFM image, and the phase boundary between metal and semiconductor could be seen clearly.

Sample C was used as an example to verify the crystal facet of GaSb attached to Ga metal for its bigger size. Good attachment[16] can be seen in TEM in Figure 2(a). In the

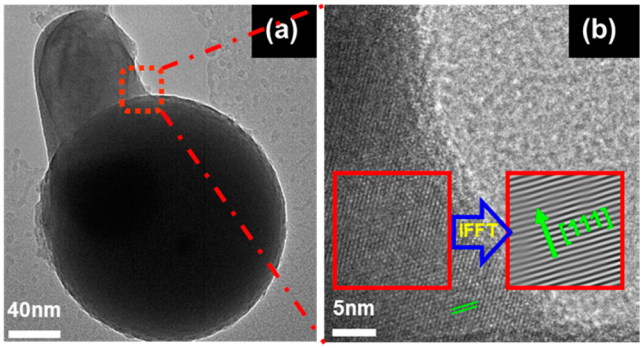


**Figure 2.** (a) Full width TEM image for sample C (Ga 15 min-Sb 30 min). (b) High resolution image for the red box with the dash line in part (a). In order to work out the crystal facet more easily, a lattice fringe image is obtained by IFFT in the red box with the solid line. And the interplanar spacing between the parallel lines is 0.352 nm.

inset in Figure 2(b), interplanar spacing (0.354 nm) between the parallel lines is similar to the interplanar crystal spacing (0.352 nm) of (111).[17] It can be concluded that the crystal facet of GaSb is the (111) crystal face, which is similar to the Au-catalyzed growth of GaSb nanowires.[18] In addition, it is also confirmed from the inverse fast fourier transformation (IFFT) images. Twin domains appear frequently in GaSb nanowires or epi-films.[19] But no twin domain or threading dislocation exists in the semiconductor part, as shown in Figure 2(b), and other locations of semiconductor parts are shown in the SI. This is due to the high migration rate on the liquid Ga metal surface before it condenses into a solid, and the stress during growth can be effectively released. Moreover, this MS hybrid has an advantage over those synthesized by directly assembling metal



DOI: 10.1021/acs.langmuir.6b00628
Langmuir 2016, 32, 4189−4193

and semiconductor particles. It is known that not all the surface facets of a semiconductor could offer appropriate work functions to form the Schottky barrier with a metal, simply because different crystal facets may have varied electronic structures, resulting in huge variations in their work functions.[20] For this reason, only when the metal is deposited on specific facets of a semiconductor can the desired Schottky barrier be formed to facilitate the migration of electrons.[21] But by assembling, the surface facet of a semiconductor attached to a metal is unfixed. In addition, it may introduce extra interface scattering which suppresses electronic transport compared with this droplet epitaxy.

The band gap of these MS hybrids is estimated from the exciton features in the absorption spectra of each size distribution, and we compare them with a GaSb epi-film on a Si(111) substrate in Figure 3. Each absorption spectrum

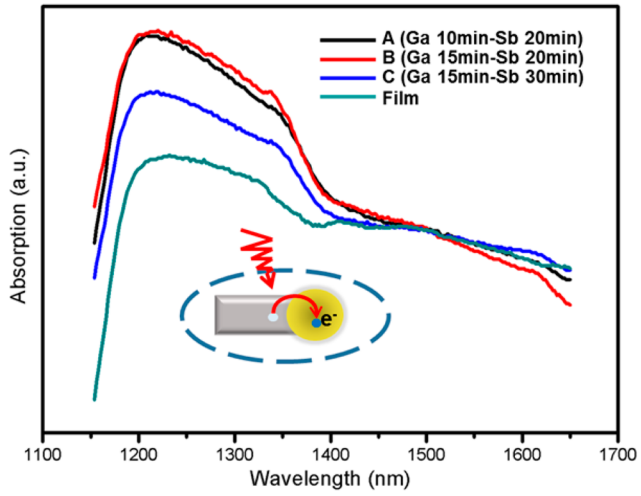


**Figure 3.** IR absorption spectrum of the MS nanohybrids and the GaSb epi-film. Absorption enhancement caused by charge transfer is shown in the schematic diagram.

consists of many absorption peaks. According to Yu's work,[22] it is reasonable to assume that the main peak around 1200 nm is the absorption for exciting electrons from the valence band (VB) to the conduction band (CB), while other peaks belong to the absorption for exciting electrons from the valence band (VB) to the defect levels between VB and CB. Compared with the GaSb epi-film, it seems that absorption enhances at the wavelength of 1150−1380 nm in MS hybrids, especially for samples A and B, in which the semiconductor part is far smaller than the metal part. Compared with other IR detection metal−semiconductor nanomaterials, Ga-GaSb MS nanohybrids own infrared absorption enhancement in the near IR-II region (wavelength 1.0−1.4 $\mu$m) and are fit for fluorescence imaging of cancer cells. Fluorescence imaging in the near IR-II is more desirable over visible (450−750 nm) and traditional near IR-I imaging (750−900 nm), owing to reduced photon scattering and deeper tissue penetration. And GaSb, whose band gap is 0.72 eV, has a good spectral response to thermal radiation of sunlight. Then Ga-GaSb MS nanohybrids can promote the conversion efficiency of thermophotovoltaic cells through this absorption enhancement.

When a semiconductor contacts a metal, a Schottky junction dependent on their work functions can be formed to affect the migration of charge carriers from the semiconductor to the metal. Herein, the work function for the metal Ga is 4.2 eV[23] and the electronic affinity for the semiconductor GaSb is 4.06 eV.[24] So energy bands in GaSb near the interface bend upward,[25] as shown in Figure 4. Thus, every absorption peak in

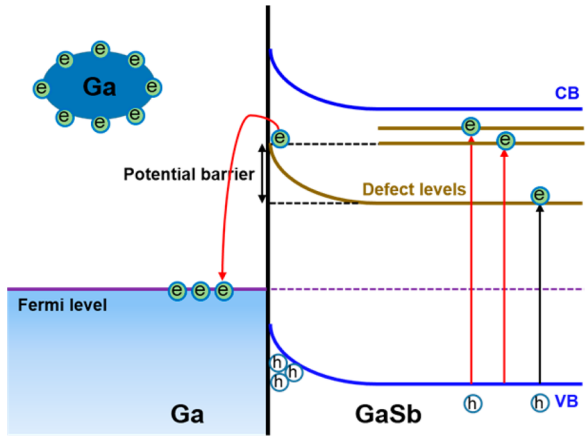


**Figure 4.** Band alignment for the MS hybrids. Charge transfer processes are marked by arrows.

Figure 3 corresponds to every energy level transition. When an electron is excited to a certain level higher than the potential barrier of the lowest defect level, it will fall into the Fermi level of metal Ga and the hole in the VB of GaSb gathers into the valence band, with the top bending upward. The concentration of exciton is thus reduced and more electrons can be excited. Therefore, absorption increases for excitation energy higher than a certain value around 1200−1380 nm due to charge separation. But absorption enhancement for sample C is not as obvious as the other two. This is mainly caused by the big size of the semiconductor part. When it is excited, so many electrons and holes are created that the valence band with its top bending upward cannot contain these holes and the surface of Ga metal will be full of electrons. Hence, the lower the proportion of semiconductor is, the stronger the absorption enhancement will be.

At the Schottky barrier formed by band bending, charge transfers to the metal, primarily from the high DOS of the semiconductor.[26] The valence band spectrum (Figure 5) near the Fermi level was used to confirm the charge transfer process. There are 2 peaks in the VB spectrum of the GaSb film.[27,28] This matches well with the theoretical calculated value, and the peak between 0 and 4 eV mainly consists of the p-like projected DOS of Ga and Sb, while it is their higher activity due to the nearest position to the Fermi level that causes these peaks in MS hybrids to decrease. Therefore, charge separation[29] at the interface of the Schottky junction and the high DOS in the semiconductor keep electrons transferring to the Fermi level of the metal. The probability of exciton recombination is reduced, and more excited electrons create more absorption.

## CONCLUSION

In summary, we have developed a successful strategy to enhance absorption through charge separation in Ga-GaSb MS nanohybrids. And it can be tuned by adjusting the size and the ratio of the metal and semiconductor. For a low ratio, the absorption enhancement reduces as the capacity for electrons on the metal surface decreases. The Schottky barrier formed by band bending drives charge separation; namely, electrons


DOI: 10.1021/acs.langmuir.6b00628
Langmuir 2016, 32, 4189−4193

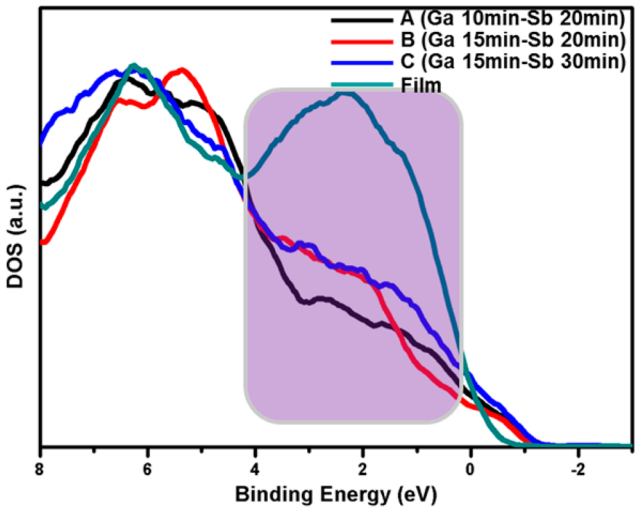


**Figure 5.** Normalized valence band spectra near the Fermi level for MS hybrids and the GaSb film. Charge transfer induces a decrease in DOS shown in the purple box.

transfer to the metal surface and holes gather into the valence band with the top bending upward. It is the high DOS in the semiconductor that keeps electrons transferring to the Fermi level of the metal. The process of electron transfer is confirmed by the VB spectrum, in which the p-like projected DOS decreases compared with the GaSb film. This will open up a broad prospect for applications in infrared detection and thermophotovoltaic cells.

## ■ ASSOCIATED CONTENT

### Supporting Information

The Supporting Information is available free of charge on the ACS Publications website at DOI: 10.1021/acs.langmuir.6b00628.

Phase diagram, detailed SEM, XRD pattern, and TEM for hybrids (PDF)

## ■ AUTHOR INFORMATION

### Corresponding Author

*E-mail: shfeng@mail.jlu.edu.cn; Fax: +86 431 85168624; Tel: +86 431 85168661.

### Notes

The authors declare no competing financial interest.

## ■ ACKNOWLEDGMENTS

This work was supported by National Natural Science Foundation of China (grants 21427802, 21131002, and 21201075) and Specialized Research Fund for the Doctoral Program of Higher Education (SRFDP grant 20110061130005).

## ■ REFERENCES

(1) Achermann, M. Exciton−plasmon interactions in metal−semiconductor nanostructures. *J. Phys. Chem. Lett.* **2010**, *1*, 2837−2843.

(2) Clavero, C. Plasmon-induced hot-electron generation at nanoparticle/metal-oxide interfaces for photovoltaic and photocatalytic devices. *Nat. Photonics* **2014**, *8*, 95−103.

(3) Shaviv, E.; Schubert, O.; Alves-Santos, M.; Goldoni, G.; Di Felice, R.; Vallee, F.; Del Fatti, N.; Banin, U.; Sönnichsen, C. Absorption properties of metal−semiconductor hybrid nanoparticles. *ACS Nano* **2011**, *5*, 4712−4719.

(4) Jiang, R.; Li, B.; Fang, C.; Wang, J. Metal/semiconductor hybrid nanostructures for plasmon-enhanced applications. *Adv. Mater.* **2014**, *26*, 5274−5309.

(5) Rycenga, M.; Cobley, C. M.; Zeng, J.; Li, W.; Moran, C. H.; Zhang, Q.; Qin, D.; Xia, Y. Controlling the synthesis and assembly of silver nanostructures for plasmonic applications. *Chem. Rev.* **2011**, *111*, 3669−3712.

(6) Zhang, W.; Saliba, M.; Stranks, S. D.; Sun, Y.; Shi, X.; Wiesner, U.; Snaith, H. J. Enhancement of perovskite-based solar cells employing core−shell metal nanoparticles. *Nano Lett.* **2013**, *13*, 4505−4510.

(7) Lin, H.; Chen, Y.; Wu, J.; Wang, D.; Chen, C. C. Carrier transfer induced photoluminescence change in metal-semiconductor core-shell nanostructures. *Appl. Phys. Lett.* **2006**, *88*, 161911.

(8) Mokari, T.; Sztrum, C. G.; Salant, A.; Rabani, E.; Banin, U. Formation of asymmetric one-sided metal-tipped semiconductor nanocrystal dots and rods. *Nat. Mater.* **2005**, *4*, 855−863.

(9) Khon, E.; Mereshchenko, A.; Tarnovsky, A. N.; Acharya, K.; Klinkova, A.; Hewa-Kasakarage, N. N.; Nemitz, I.; Zamkov, M. Suppression of the plasmon resonance in Au/CdS colloidal nanocomposites. *Nano Lett.* **2011**, *11*, 1792−1799.

(10) Wang, L.; Ge, J.; Wang, A.; Deng, M.; Wang, X.; Bai, S.; Li, R.; Jiang, J.; Zhang, Q.; Luo, Y. Designing p-type semiconductor−metal hybrid structures for improved photocatalysis. *Angew. Chem., Int. Ed.* **2014**, *53*, 5107−5111.

(11) Ding, X.; Liow, C. H.; Zhang, M.; Huang, R.; Li, C.; Shen, H.; Liu, M.; Zou, Y.; Gao, N.; Zhang, Z. Surface plasmon resonance enhanced light absorption and photothermal therapy in the second near-infrared window. *J. Am. Chem. Soc.* **2014**, *136*, 15684−15693.

(12) Kunrugsa, M.; Kiravittaya, S.; Panyakeow, S.; Ratanathammaphan, S. Effect of Ga deposition rates on GaSb nanostructures grown by droplet epitaxy. *J. Cryst. Growth* **2014**, *402*, 285−290.

(13) Elborg, M.; Noda, T.; Mano, T.; Jo, M.; Sakuma, Y.; Sakoda, K. Self-assembly of Ga droplets attached to GaAs quantum dots. *J. Cryst. Growth* **2013**, *378*, 53−56.

(14) Kern, W. The evolution of silicon wafer cleaning technology. *J. Electrochem. Soc.* **1990**, *137*, 1887−1892.

(15) Wang, Z. M.; Liang, B.; Sablon, K. A.; Lee, J.; Mazur, Y. I.; Strom, N. W.; Salamo, G. J. Self-organization of InAs quantum-dot clusters directed by droplet homoepitaxy. *Small* **2007**, *3*, 235−238.

(16) Chen, Y.; Zeng, D.; Cortie, M. B.; Dowd, A.; Guo, H.; Wang, J.; Peng, D. L. Seed-induced growth of flower-like Au−Ni−ZnO metal−semiconductor hybrid nanocrystals for photocatalytic applications. *Small* **2015**, *11*, 1460−1469.

(17) Hocevar, M.; Immink, G.; Verheijen, M.; Akopian, N.; Zwiller, V.; Kouwenhoven, L.; Bakkers, E. Growth and optical properties of axial hybrid III−V/silicon nanowires. *Nat. Commun.* **2012**, *3*, 1266.

(18) Yang, Z.; Han, N.; Fang, M.; Lin, H.; Cheung, H. Y.; Yip, S.; Wang, E. J.; Hung, T.; Wong, C. Y.; Ho, J. C. Surfactant-assisted chemical vapour deposition of high-performance small-diameter GaSb nanowires. *Nat. Commun.* **2014**, *5*, 5249.

(19) Dasgupta, N. P.; Sun, J.; Liu, C.; Brittman, S.; Andrews, S. C.; Lim, J.; Gao, H.; Yan, R.; Yang, P. Semiconductor nanowires−synthesis, characterization, and applications. *Adv. Mater.* **2014**, *26*, 2137−2184.

(20) Li, R.; Zhang, F.; Wang, D.; Yang, J.; Li, M.; Zhu, J.; Zhou, X.; Han, H.; Li, C. Spatial separation of photogenerated electrons and holes among {010} and {110} crystal facets of $BiVO_4$. *Nat. Commun.* **2013**, *4*, 1432.

(21) Nelson, J. *The physics of solar cells*; World Scientific: 2003; Vol. *1*.

(22) Yu, H.; Li, J.; Loomis, R. A.; Wang, L. W.; Buhro, W. E. Two- versus three-dimensional quantum confinement in indium phosphide wires and dots. *Nat. Mater.* **2003**, *2*, 517−520.

(23) Michaelson, H. B. The work function of the elements and its periodicity. *J. Appl. Phys.* **1977**, *48*, 4729−4733.



DOI: 10.1021/acs.langmuir.6b00628
*Langmuir* 2016, 32, 4189−4193

(24) Sasaki, A. Effective-mass superlattice. *Phys. Rev. B: Condens. Matter Mater. Phys.* **1984**, *30*, 7016.
(25) Bachrach, R.; Bianconi, A. Interface states at the Ga−GaAs interface. *J. Vac. Sci. Technol.* **1978**, *15*, 525−528.
(26) Brillson, L. The structure and properties of metal-semiconductor interfaces. *Surf. Sci. Rep.* **1982**, *2*, 123−326.
(27) Li, C.; Lu, K.; Wang, Y. Electronic structure of liquid gallium antimonide tested with x-ray absorption near-edge-structure spectroscopy. *J. Phys.: Condens. Matter* **1999**, *11*, 3013.
(28) Gu, T.; Qin, J.; Bian, X.; Xu, C.; Qi, Y. Ab initio molecular dynamics simulations of liquid structure change with temperature for a GaSb alloy. *Phys. Rev. B: Condens. Matter Mater. Phys.* **2004**, *70*, 245214.
(29) Mongin, D.; Shaviv, E.; Maioli, P.; Crut, A. l.; Banin, U.; Del Fatti, N.; Vallée, F. Ultrafast photoinduced charge separation in metal−semiconductor nanohybrids. *ACS Nano* **2012**, *6*, 7034−7043.



DOI: 10.1021/acs.langmuir.6b00628
*Langmuir* 2016, 32, 4189−4193